ORGANOMETALLICS
Article
Cite This: Organometallics XXXX, XXX, XXX−XXX
pubs.acs.org/Organometallics

Intriguing Behavior of an Apparently Simple Coupling Promoter Ligand, $PPh_2(p\text{-}C_6H_4{-}C_6F_5)$, in Their Pd Complexes

María Pérez-Iglesias,[‡] Rebeca Infante,[‡] Juan A. Casares,[*] and Pablo Espinet[*]

IU CINQUIMA/Química Inorgánica, Facultad de Ciencias, Universidad de Valladolid, 47011 Valladolid, Spain

Supporting Information

ABSTRACT: Ligand $PPh_2(p\text{-}C_6H_4{-}C_6F_5)$, $\mathbf{L^{HF}}$, is an example of monodentate biphenyl phosphine that allows for cis coordination of two phosphines to Pd, as in complex *cis*-$[PdPf_2Pd(\mathbf{L^{HF}})_2]$ (**A**) (Pf = C_6F_5). At 25 °C, complex **A** undergoes easy reductive elimination to decafluorobiphenyl and, competitively, isomerizes to *trans*-$[Pd(C_6F_5)_2Pd(\mathbf{L^{HF}})_2]$ via functionally three-coordinate intermediates *cis*-$[PdPf_2(\mathbf{L^{HF}})(S)]$ with the fourth position empty or weakly protected (S= THF, OH_2, or π-aryl). Unexpectedly, the direct reductive $C_6F_5{-}C_6F_5$ elimination is faster from the four-coordinate complex **A** than from the intermediates with only one strong $\mathbf{L^{HF}}$. The reason for this is that two cis $\mathbf{L^{HF}}$ ligands play the role of a chelate with a large bite angle and some tetrahedral distortion. As a matter of fact, using $\mathbf{L^{HF}}$ in excess (Pd:L ≪ 1:2), a Pf−Pf coupling barrier $\Delta G^{\ddagger}_{Pf-Pf}$ = 23.1 kcal·mol^{-1} is measured, which ranks its efficiency for coupling and formation of the corresponding Pd^0 catalyst as better than XantPhos or PhPEWO-F and about the same as ^{t}BuBrettPhos. On the other hand, complex $(\mu\text{-}Cl)_2[Pd_2Rf_2(\mathbf{L^{HF}})_2]$ (**B**) (Rf = $C_6F_3Cl_2$ = 3,5-dichloro-2,4,6-trifluorophenyl), obtained by reaction of $(\mu\text{-}Cl)_2[Pd_2Rf_2(tht)_2]$ (tht = tetrahydrothiophene) with $\mathbf{L^{HF}}$, presents in the ^{19}F NMR COSY spectrum a very intriguing *through-space* coupling pattern of the F_{ortho} atoms of the C_6F_5 group in $\mathbf{L^{HF}}$ and the 3-5-$C_6F_3Cl_2$ group on Pd. The intermittent coupling mechanism proposed is based on the switching of $\pi{-}\pi$-stacking of C_6F_5 from one Ph group to another Ph group of $\mathbf{L^{HF}}$, which gives rise to enantiomers at the chiral P atom. Rotation around the P−biphenyl bond under hindered rotation around the $C{-}C_6F_5$ bond produces the intriguing selective coupling observed.

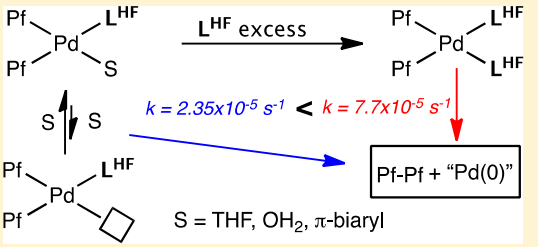

INTRODUCTION

Recently, we reported a procedure to evaluate the ability of different ligands to facilitate difficult C−C couplings in Pd. It uses the so-called *couplimeter* complex *cis*-$[PdPf_2(THF)_2]$ (**1**) (Pf = C_6F_5; THF = tetrahydrofuran), which allows $\Delta G^{\ddagger}_{Pf-Pf}$, the activation energy of the coupling step producing Pf−Pf upon addition of the ligand, to be measured experimentally. This leads to ranking the ligands according to their corresponding $\Delta G^{\ddagger}_{Pf-Pf}$ values.[1] Ligands ^{t}BuXPhos ($\Delta G^{\ddagger}_{Pf-Pf}$ = 21.8 kcal·mol^{-1} at 0 °C) and PhPEWO-F ($\Delta G^{\ddagger}_{Pf-Pf}$ = 22.3 kcal·mol^{-1} at 25 °C) are among the most active ligands for coupling at 0−25 °C, certainly more efficient than the typical large bite angle ligand XantPhos ($\Delta G^{\ddagger}_{Pf-Pf}$ = 24.2 kcal·mol^{-1} at 25 °C). The coupling product of the reaction, Pf−Pf, is only hardly reactive; hence, complex **1** can be used as a convenient precursor to generate $[Pd^0L_n]$ catalysts in situ.[1]

The ability of RPEWO-F ligands to induce C−C coupling is due to the presence of a strongly electron-withdrawing double bond: it lowers the coupling activation energy by withdrawing the increasing electron density on Pd as the reduction from Pd^{II} to Pd^0 progresses.[2−6] In fact, the ligand PhPEWO-F, shown in Figure 1, left, induces much faster coupling than the related nonfluorinated PhPEWO-H, with H atoms instead of F atoms, because its olefin function is a stronger EWO group.[1]

In X-ray diffraction structures of "three-coordinate" palladium complexes with biphenyl phosphines, one carbon atom of the distal aryl group is located at a short distance of the Pd atom; similarly, in some PEWO-F complexes, one carbon atom of the olefin group is a short distance from the Pd atom.[7] These common features, suggestive of some similarity of the respective EWO or biphenyl interactions with the Pd center, call for more detailed examination.

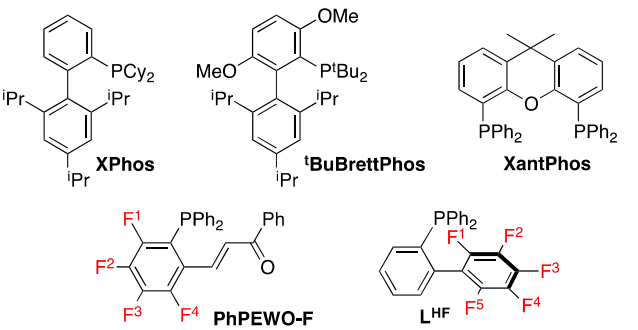

Figure 1. Structures of ^{t}BuXPhos, XantPhos, and the partially fluorinated PhPEWO-F and $PPh_2(o\text{-}C_6H_4{-}C_6F_5)$ ($\mathbf{L^{HF}}$) ligands.

The electron density on the biphenyl of PR_2(biaryl) ligands has been reported to strongly affect the rate of reductive elimination from palladium(II) complexes. The frequent

Received: July 8, 2019

Downloaded via MACQUARIE UNIV on August 29, 2019 at 22:15:01 (UTC).
See https://pubs.acs.org/sharingguidelines for options on how to legitimately share published articles.

© XXXX American Chemical Society

DOI: 10.1021/acs.organomet.9b00460
Organometallics XXXX, XXX, XXX−XXX

presence of electron-donating groups on the distal arene is detrimental for the reductive elimination rate.[8] We hypothesized that ligand fluorination at the distal aryl of the biphenyl might increase their similarity with our PEWO-F ligands. Although some partially fluorinated biaryl phosphines have already been reported and their catalytic performance was not particularly good when compared with that of nonfluorinated analogues,[9−13] these results are not necessarily informative about the reductive elimination step. In this context, we decided to synthesize and examine the behavior of a new PR_2(biaryl) ligand fluorinated at the distal aryl group, $\mathbf{L^{HF}}$ (Figure 1, right) and immediately set to estimate its coupling potential, measuring $\Delta G^{\ddagger}_{Pf-Pf}$ with the standard protocol reported in ref 1. Unexpectedly, $\mathbf{L^{HF}}$ behaved very differently from other biphenyl phosphines such as ^{t}BuXPhos or diphosphines such as XantPhos that were previously submitted to this protocol.[1] In these, the addition of free ligand to *cis*-[$PdPf_2(THF)_2$] above the L:Pd = 1:1 ratio did not alter the coupling rate measured for L:Pd = 1:1. In contrast, for $\mathbf{L^{HF}}$, successive additions of free ligand over the 1:1 ratio produced progressively attenuated increases of the coupling rate. This effect ceased for a L:Pd ratio well above 2:1, when the coupling reaction reached was about 3-fold the initial one. This behavior is compatible with the formation of a mixture of [$PdPf_2(\mathbf{L^{HF}})$] and *cis*-[$PdPf_2(\mathbf{L^{HF}})_2$], at variance with ^{t}BuXPhos or XantPhos, which form only *cis*-[$PdPf_2(\mathbf{L})$] in both cases. Yet, the accelerating effect upon addition of free ligand is unusual on an isolated coupling process: deceleration or no effect is usually observed for Pd^{II}.[14] This work aims at supporting and explaining in detail the different behavior of $\mathbf{L^{HF}}$ compared to that of many other biarylphosphines.

RESULTS AND DISCUSSION

Synthesis of the Ligand. $\mathbf{L^{HF}}$ was synthesized from 2′-lithium-2,3,4,5,6-pentafluoro-1,1′-biphenyl and PPh_2Cl and was chemically characterized in solution by ^{1}H, ^{19}F, ^{31}P, and ^{13}C NMR as well as computationally. Its ^{19}F NMR spectrum shows the typical AA′XX′Z spin system found for symmetrical C_6F_5 groups. The $^{31}P\{^1H\}$ NMR signal is a triplet by coupling to the F^1 and F^5 ortho atoms (J_{F-P} = 27 Hz) as shown by a $^{19}F-^{31}P$ HSQC correlation. This supports that a fast rotation of the fluoraryl group around the C−C bond is taking place in solution at 25 °C. Values of about 30 Hz are typical for $^3J(F_{ortho}-P)$ couplings (e.g., $P(C_6F_5)_3$ or $P(C_6F_5)_2Ph$),[15,16] and smaller values are found in other fluoroaryl phosphines such as PhPEWO-F ($^3J_{F-P} \approx 15$ Hz)[17] and in fluoroalkylphosphines.[18] Coupling constants $^5J(^{19}F-^{31}P)$ are usually very small or unobservable, but exceptions are dicyclohexyl(2′,6′-difluoro-[1,1′-biphenyl]-2-yl)-phosphine (J_{F-P} = 24 Hz) and $\mathbf{L^{HF}}$.[11] The simplest explanation for these anomalous values is that there is some "through-space" coupling contribution to coupling, strongly dependent on the distance between nuclei,[19−21] in addition to the ^5J scalar coupling contribution. In the palladium complexes of $\mathbf{L^{HF}}$ (see below), this $^{19}F-^{31}P$ coupling is not observed.

The structure of $\mathbf{L^{HF}}$ in the gas phase has been calculated by DFT (wB97XD/6-31G// wB97XD /SDD, details in Supporting Information (SI)). Its most stable atropisomer is shown in Figure 2a and shows the biaryl group roughly oriented toward the lone pair of the P atom. In this conformation, one of the $P\cdots F_{ortho}$ distances is as short as 3.305 Å, close enough to display a through-space contribution to coupling. A Pf−Ph π-stacking is observed, with $Pf_{centroid}-Ph_{centroid}$ distance = 3.654 Å. The less stable atropisomer, shown in Figure 2b, adopts a conformation with the biaryl roughly opposite to the lone electron pair of the phosphorus atom. In this conformation, the two $P\cdots F_{ortho}$ distances are 4.210 and 4.227 Å, minimizing the through-space contribution to coupling. Note also in Figure 2b the existence of a very efficient Pf−Ph π-stacking, with $Pf_{centroid}-Ph_{centroid}$ distance = 3.426 Å. As far as this π-stacking is operative, it makes the P atom temporarily chiral; if the Pf−Ph π-stacking is moved to the other Ph group, it produces the other enantiomer. This is relevant later in the $\mathbf{L^{HF}}$ Pd complexes.

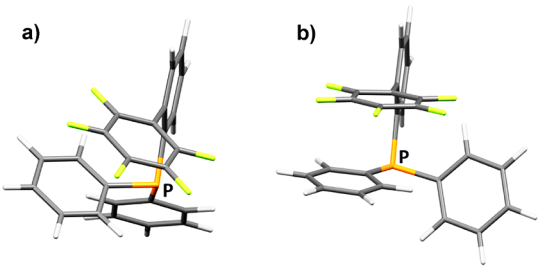

Figure 2. (a) Most stable conformation of free $\mathbf{L^{HF}}$. (b) Less stable conformation for free $\mathbf{L^{HF}}$, which can be preferred in complexes.

Coordination of $\mathbf{L^{HF}}$ to Palladium(II). Scheme 1 shows the syntheses of complexes **2**−**5**, prepared for the study. Other complexes appearing or being formed in solution are discussed later, as they are required.

Scheme 1. Synthesis of Complexes 2−5

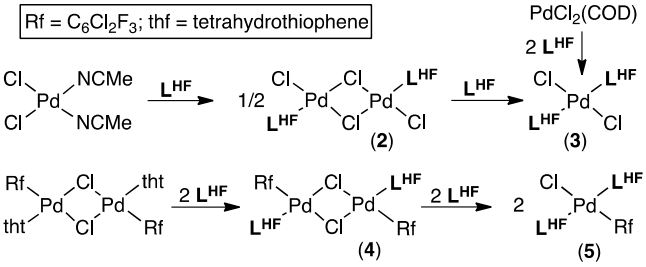

Ligand $\mathbf{L^{HF}}$ (1 eq per palladium) reacts with $PdCl_2(NCMe)_2$ to produce the dimer $(\mu\text{-}Cl)_2[PdCl(\mathbf{L^{HF}})]_2$ (**2**). The use of excess of $\mathbf{L^{HF}}$ yields the monomer *trans*-[$PdCl_2(\mathbf{L^{HF}})_2$] (**3**), which is better obtained by the reaction of [$PdCl_2$(1,5-COD)] with 2 eq of $\mathbf{L^{HF}}$. Both complexes show in the IR spectrum the typical $\nu(^{35}Cl-Pd)$ stretching band of terminal Pd−Cl bonds close to 360 cm^{-1} and the $\nu(^{37}Cl-Pd)$ shoulder at 353 cm^{-1}. The dimer shows additional absorptions for bridging chlorides, at lower wavenumbers (304 and 294 as well as 272 and 264 cm^{-1}).

The X-ray structure of **2** shows a coplanar arrangement of their two square-planar halves.[22] The $\mathbf{L^{HF}}$ conformation is somehow similar to the most stable conformation of the free phosphine, at least in the solid state: the modest out-of-plane steric hindrance of the chloro ligands allows for the distal pentafluorophenyl group of the biphenyl to occupy the space above and below the Pd coordination planes, lying almost parallel to them (Figure 3). Bond distances and angles are conventional, but it is worth noting the short distance from Pd to the C_{ipso} (C1) of Pf (3.142 Å). This kind of biphenyl arrangement with similar distances has been studied for linear

DOI: 10.1021/acs.organomet.9b00460
Organometallics XXXX, XXX, XXX−XXX

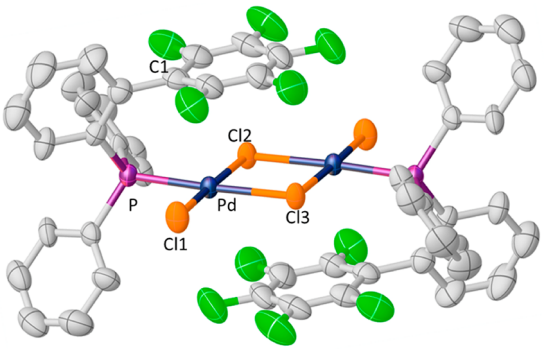

Figure 3. ORTEP diagram (50%) of $(\mu\text{-Cl})_2[Pd_2Cl_2(\mathbf{L}^{HF})_2]$ (**2**). Bond distances (Å): Pd−P = 2.226; Pd−C1 = 3.141; Pd−Cl1 = 2.272; Pd−Cl2 = 2.411; Pd−Cl3 = 2.320.

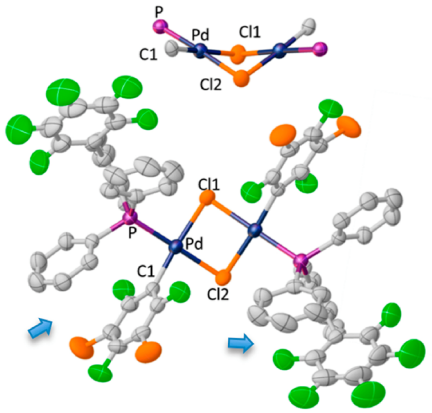

Figure 4. ORTEP diagram (50%) of $(\mu\text{-Cl})_2[PdRf(\mathbf{L}^{HF})]_2$ (**4**·$CHCl_3$, disordered $CHCl_3$ omitted for clarity). Bond distances (Å): Pd−C1 = 1.995; Pd−P = 2.262; Pd−Cl1 = 2.407; Pd−Cl2 = 2.388. Blue arrows point to π−π-stacking zones: Ph−Rf stacking distance between centroids = 3.117 Å; Ph−Pf stacking distance between centroids = 3.212 Å. Above: Another view of the angular arrangement of the two coordination square planes.

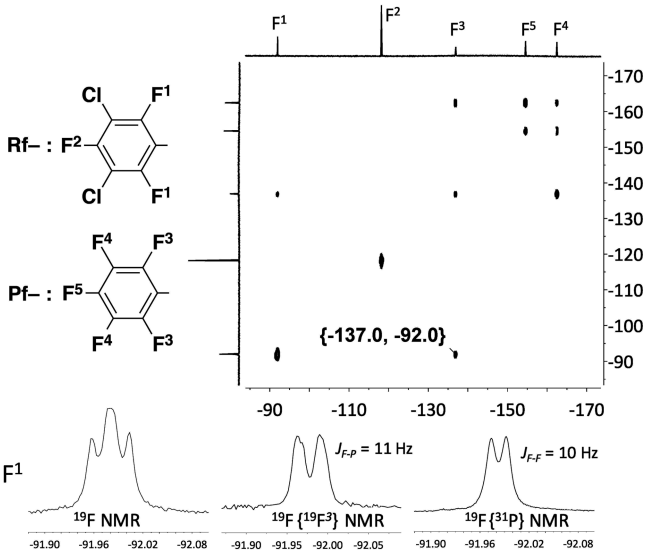

Figure 5. Above: ^{19}F-COSY of **4** in $CDCl_3$ at 25 °C. Below: Effect of selective irradiations on the deceptive F^1 triplet.

Au^I complexes (note that Au^I and Pd^{II} have almost identical radii).[23,24]

The $^{31}P\{^1H\}$ NMR spectrum of **2** at 25 °C displays one singlet ($\nu_{1/2}$ = 5 Hz), where no $^5J_{F-P}$ is observed. In the ^{19}F NMR spectrum, the two F_{ortho} nuclei and the two F_{meta} nuclei are equivalent, meaning that there is fast rotation of the C_6F_5 group about the C−C bond. Obviously, this requires that the Pd coordination plane and the distal Pf group, observed in close parallel arrangement in the X-ray structure, get separated in solution in order to allow for rotation around the P−C and C−Pf bonds. The coalescence temperature is not still reached down to −30 °C, suggesting that the rotational barriers in **2** must be very small.

Similar ^{19}F NMR behavior is found for the monomeric *trans*-$[PdCl_2(\mathbf{L}^{HF})_2]$ (**3**). The trans structure of **3** was assigned based on the observation in the IR spectrum of $\nu_{assim}(Pd-^{35}Cl)$ and $\nu_{assim}(Pd-^{37}Cl)$ bands at 360 and 351 cm^{-1}, respectively.

The dimeric complex $(\mu\text{-Cl})_2[PdRf(\mathbf{L}^{HF})]_2$ (**4**) (Rf = $C_6F_3Cl_2$, 3,5-dichloro-2,4,6-trifluorophenyl) is easily prepared by reacting the precursor $(\mu\text{-Cl})_2[PdRf(tht)]_2$, (tht = tetrahydrothiophene) with $\mathbf{L}^{HF}$ (Pd:$\mathbf{L}^{HF}$ = 1:1). It shows IR bridging chloride bands at lower wavenumbers, at 306 and 296 as well as 284 and 271 cm^{-1}. The X-ray structure of **4**·$CHCl_3$ is shown in Figure 4. The complex displays two square-planar units making a 135.8° dihedral angle at the $(\mu\text{-Cl})_2$ edge. Each square-planar complex has conventional Pd−Cl (2.388 Å), Pd−P (2.262 Å), and Pd−C (1.995 Å) distances and angles and no significant distortion from planarity.[25] The Rf group imposes steric constraints at the coordination plane zone, which force a conformational change on $\mathbf{L}^{HF}$, pushing the pentafluorophenyl ring away from the palladium coordination plane. This different rearrangement from **2** does not alter significantly the bond distances and angles at the coordination plane, but the $\mathbf{L}^{HF}$ coordinated ligand is involved in two relatively strong π-stacking interactions: one *intraligand* Ph−Pf at 3.117 Å between centroids, reminiscent of what happens in the free ligand and one *extraligand* Ph−Rf at 3.212 Å.

The ^{19}F NMR spectrum of compound **4** (see Figure 5 for spectra and F labeling) is surprising and intriguing. It shows the expected number of signals for an Rf group with chemically equivalent halves (two signals in a ratio of 2:1 for F^1 and F^2) and for a Pf group with chemically equivalent halves (three signals in a 2:2:1 ratio for F^3:F^4:F^5). Even assuming that the two Pd coordination planes of the dimer will fast average to coplanar in the NMR time scale, the chemical equivalence of the two F^1 atoms in the Rf group is something unusual: It is very well established that the rotation of Rf groups about the C−Pd bond is severely restricted in complexes with nonflat ligands that are not easily dissociable (e.g., PPh_3) cis-coordinated relative to Rf.[26] Hence, because the Pd coordination plane of **4** is not a symmetry plane for the molecule, the two F^1 atoms should be anisochronous.

The $^{31}P\{^1H\}$ NMR spectrum of **4** shows a triplet ($^4J_{F-P}$ = 11 Hz), as expected for a phosphine cis to Rf, provided that the two F^1 were equivalent. Consequently, a mechanism different from the hindered rotation about the Rf−Pd bound must exist.

The ^{19}F-COSY of **4** in $CDCl_3$ at 25 °C (Figure 5) confirms the internal F−F coupling between the fluorine nuclei of Pf and the absence of internal F−F coupling in Rf. Additionally, it reveals the existence of unexpected (looking at the X-ray structure in Figure 4) through-space J_{F-F} coupling ($J \approx 10$ Hz) between F^1 and F^3.[21] This produces a deceptive triplet for the F^1 signal. Double irradiation experiments ($^{19}F\{^{31}P\}$ and $^{19}F\{^{19}F^3\}$) reveal that this deceptive multiplicity is due to coupling

DOI: 10.1021/acs.organomet.9b00460
Organometallics XXXX, XXX, XXX−XXX

to the phosphorus ($^4J_{F-P}$ = 11 Hz) and to only one F^3 atom ($J \approx 10$ Hz) of the Pf group (J_{F-F} = 10 Hz) (note that paradoxically both F^3 atoms are spectroscopically equivalent). Thus, the equivalence mechanism has to be able to explain the through-space F^1-F^3 coupling involving only one pair of atoms at a time and still justify the chemical equivalence of the two halves of the Pf and Rf groups. In other words: what kind of fluxional process produces chemical equivalence of the two F^3 and still does not produce coupling of each F^1 to both F^3? This suggests that the process must be explained under restricted rotation of Pf around the Pf–C bond or at least a higher rotational barrier than the fluxionality leading to the through-space couplings observed.

A closer inspection of the X-ray structure of complex **4** shows that the π-stacking interactions noted above make the P atom a chiral center. The choice of one or the other Ph ring to interact with the Pf group determines the P conformation. This is already seen in the less stable atropisomer of free $\mathbf{L^{HF}}$, where the lone pair plays the role of Pd in the complex (Figure 2b).

In the complex, the hindrance produced by the $\pi-\pi$-stacked chiral conformation allows that only one F^3 can get close to the F^1 at that side of the coordination plane. The NMR behavior observed ^{19}F can then be explained as associated with the switching between enantiomers. The slippage of the Pf group from Ph^1 to Ph^2, involving progressive weakening of the $\pi-\pi$-stacking with Ph^1 and strengthening of the $\pi-\pi$-stacking with Ph^2, occurs along a crowded pathway where rotation around the Pf–C bond is restricted. In the new isomer, the Pf group is at the other side of the coordination plane (rotation around the Pd–P bond is forced in the same movement), and it is the other F^1/F^3 pair that can get close to produce through-space coupling. It is interesting to note the fact that the rotation around the P–C(biphenyl) bond occurs with the restriction that the Pf–C rotation cannot occur, whereas the rotation of the phosphine around the P–Pd bond maintains the hindrance to rotation of the Rf group around the Rf–Pd bond (Scheme 2).

Scheme 2. Fluxional Process Observed for Complexes 4 and 5[a]

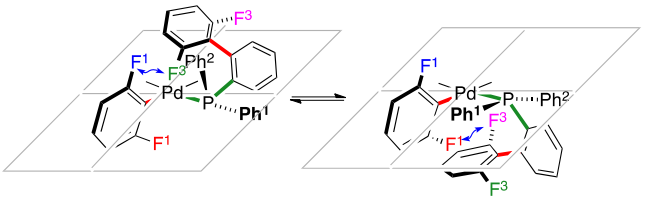

[a]For simplicity, only the F_{ortho} atoms (F^1 and F^3) are represented. Green bonds indicate allowed rotations, and red bonds indicate restricted rotations.

As the spin–spin connection is not lost along the fluxional movement because there is no phosphine dissociation, the observed $J \approx 10$ Hz is the time averaged value varying along the fluxional process from a nondetermined maximum value to zero. As far as we are aware, nothing like this racemization mechanism associated with $\pi-\pi$-stacking slippage has been reported before, although it must be taking place in many related systems, being unobservable or passing unnoticed.

Complex **4** reacts with an excess of $\mathbf{L^{HF}}$ to produce *trans*-$[PdRfCl(\mathbf{L^{HF}})_2]$ (**5**). The NMR spectra of **5**, following the same clockwork fluxional behavior, behave as just discussed for **4** with a small variation due to the presence of two $\mathbf{L^{HF}}$ ligands: The ^{31}P NMR shows a triplet due to the coupling with two F^1 atoms, and the F^1 signals appear as deceptive quintuplets in the ^{19}F NMR spectrum because of coupling of two P atoms and coincidence of J_{F-P} and J_{F-F} values.

Reductive Elimination Reaction. The reductive elimination of $[PdPf_2(THF)_2]$ (**1**) was studied in toluene by adding different proportions of $\mathbf{L^{HF}}$ and monitoring the formation of Pf–Pf by ^{19}F NMR. The behavior was anomalous to the case of ^{t}BuXPhos, where the coupling rate was independent of the Pd:L used.[1]

The study required previously being able to identify in solution some complexes by NMR: *cis*-$[PdPf_2(\mathbf{L^{HF}})_2]$ (**6**), which could also be isolated and its structural details studied by a combination of defective X-ray diffraction results asa base for DFT calculation; *trans*-$[PdPf_2(\mathbf{L^{HF}})_2]$ (**8**), which was also prepared as a stable solid; and a number of complexes with just one $\mathbf{L^{HF}}$ *per* Pd, some of them observable under appropriate conditions, which are species considered *functionally three-coordinate*.[27] In our case, these can have the fourth coordination position empty or weakly protected by interaction with the distal aryl of the biphenyl or with an easily displaceable molecule (THF, OH_2, which are weak ligands for soft Pd^{II}) so that their conversion to that empty position is not needed or requires very little energy. This means that for kinetic purposes, they can be approximated globally, with acceptable approximation, as all being the same species *cis*-$[PdPf_2(\mathbf{L^{HF}})(S)]$ (**7**). In this respect, no assumption needs to be made on whether they really dissociate to the real *three-coordinate* or they couple directly from the tetracoordinate species **7** with only one $\mathbf{L^{HF}}$ ligand. The kinetic treatment is discussed in detail in the Supporting Information.

Addition to complex **1** in toluene of excess $\mathbf{L^{HF}}$ produces immediately *cis*-$[PdPf_2(\mathbf{L^{HF}})_2]$ (**6**). This complex is unstable in solution at room temperature (undergoing reductive elimination of Pf–Pf), but it can be crystallized from toluene at −35 °C as a colorless solid. The poor quality of the crystals obtained affects the quality of the X-ray diffraction data and the reliability of the structure of **6**·toluene obtained. This defective structure (suppressing the toluene molecule) was DFT optimized in the gas phase, and the valuable geometrical information obtained (coincident with the X-ray data except for moderate variations in bond distances and angles) is shown in Figure 6. The structure confirms that two $\mathbf{L^{HF}}$ ligands can occupy cis positions in Pd. The complex displays tetrahedrally

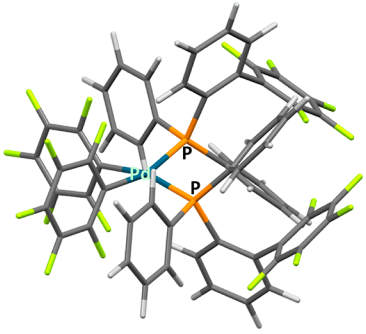

Figure 6. DFT capped-stick structure of *cis*-$[PdPf_2(\mathbf{L^{HF}})_2]$, optimized from a defective X-ray solution of **6**·toluene (see SI). It shows some tetrahedral distortion of the square plane induced by the biaryl substituents on P.

DOI: 10.1021/acs.organomet.9b00460
Organometallics XXXX, XXX, XXX–XXX

distorted square-planar cis geometry (the two trans Pf−Pd−P angles are 164.0°). A C_2 axis makes the two Pf groups and the two $\mathbf{L}^{HF}$ phosphines symmetry equivalent. The conformation of $\mathbf{L}^{HF}$ shows the biphenyl with its Pf ring away from the palladium plane, as expected. The repulsion between the two bulky phosphine ligands forces a P−Pd−P angle of 104.8°, a bit larger than the same angle in $[PdRf_2(XantPhos)]\cdot 2CH_2Cl_2$ (103.5°).[28] Thus, the effect of the two voluminous phosphines forcing a large P−Pd−P angle is higher than that of XantPhos (a typical chelate with a large bite angle). Consistently, the C−Pd−C angle in **6** (81.21°) is smaller than 90° but a bit larger than in the rigid complex with XantPhos (79.6°), because in the case of XantPhos, the planar square plane is less distorted. The coupling promoter effect of ligands with large bite angles is well-known. In theoretical calculations,[14a] not only the reduction of the C−Pd−C angle but also a tetrahedral distortion of the square plane are features observed in the structural evolution during C−C coupling in case that the four ligands are conserved during the reaction.[29] Both features are incipiently observed for *cis*-$[PdPf_2(\mathbf{L}^{HF})_2]$, whereas the tetrahedral distortion effect is not observed in the complex with XantPhos, and perhaps, this explains the significantly higher coupling efficiency of $2\mathbf{L}^{HF}$ ($\Delta G^{\ddagger}_{Pf-Pf}$ = 23.1 kcal·mol^{-1} at 25 °C, see later) compared to that of XantPhos ($\Delta G^{\ddagger}_{Pf-Pf}$ = 24.2 kcal·mol^{-1} at 25 °C), in spite of the smaller C−Pd−C angle defined by XantPhos in its ground state structure.

On the other hand, *trans*-$[PdPf_2(\mathbf{L}^{HF})_2]$ (**8**) was easily prepared by reaction of *cis*-$[PdPf_2(SMe_2)_2]$[30] with a stoichiometric amount of $\mathbf{L}^{HF}$ in dichloromethane and isolated as a stable solid (details in SI). With the spectroscopic data of **1**, **6**, and **8** in hand, the evolution of the reactions **1** + $n\mathbf{L}^{HF}$ could be studied.

The NMR spectra of mixtures of **1** and $\mathbf{L}^{HF}$ in different proportions, prepared and recorded at −20 °C in order to prevent coupling, reveal the existence of the complexes and equilibria shown in Scheme 3. Above 0 °C, two processes are observed: the reductive elimination to Pf−Pf and the isomerization of **6** to *trans*-$[PdPf_2(\mathbf{L}^{HF})_2]$ (**8**). The reductive elimination behavior at 25 °C can be analyzed based on the existence of these equilibria and the kinetic monitoring of the processes in different $\mathbf{L}^{HF}$:Pd ratios. Data related to the characterization of these equilibria at different temperatures are discussed in the SI.

Scheme 3. Equilibria Observed in Toluene Solution at −20 °C and Evolution to 8 at 0 °C[a]

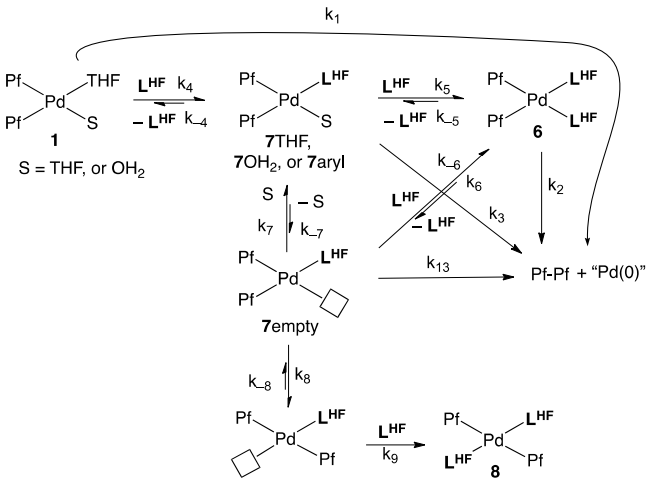

[a]Note that "dry" toluene contains a small amount of residual water (about 5 pm).[31] The initial complex **1** is represented as *cis*-$[PdPf_2(THF)(S)]$ to include molecules where THF has been substituted by water in the solvent. For details of the kinetic study, see SI.

(1) With a large excess of $\mathbf{L}^{HF}$($[\mathbf{L}^{HF}]$:$[PdPf_2(THF)_2] \geq$ 4:1), initially the only significant Pd species in solution is *cis*-$[PdPf_2(\mathbf{L}^{HF})_2]$ (**6**, red dots) plus at least 2 eq of free $\mathbf{L}^{HF}$ and 2 eq of free THF). The reductive elimination to Pf−Pf (blue dots) is the only process observed at 25 °C. The concentration/time plots (Figure 7 fit very well first order kinetics (k_{elim} = 7.7 × 10^{-5} s^{-1}, $\Delta G^{\ddagger}_{Pf-Pf}$ = 23.1 kcal·mol^{-1} at 25 °C), and the observed rate does not change when increasing the concentration of $\mathbf{L}^{HF}$, confirming that the coupling is taking place on the four-coordinated complex, induced by the large bite angle defined by the two phosphines in cis.

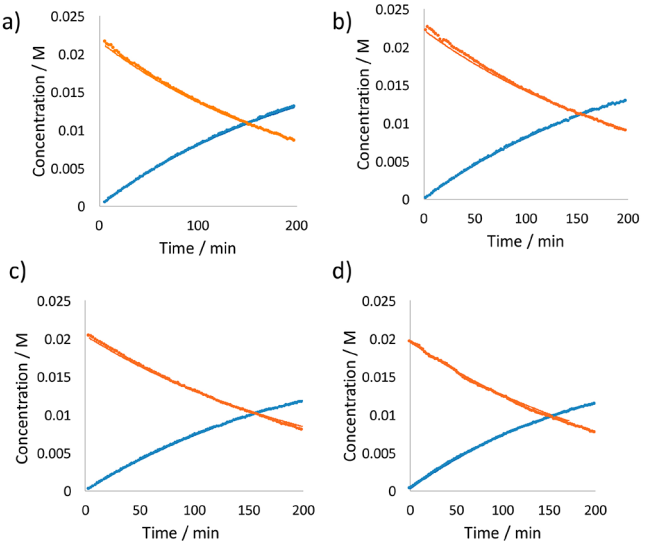

Figure 7. Concentration/time plots and best least-squares fitting (continuous line) for reductive elimination of **6** in toluene under selected concentrations of $\mathbf{L}^{HF}$ at 298 K. Red dots: *cis*-$[PdPf_2(\mathbf{L}^{HF})_2]$ (**6**); blue dots: Pf−Pf. Starting conditions: (a) [**1**] = 0.02 M + $[\mathbf{L}^{HF}]$ = 0.08 M (1:4), k_{obs} = 7.7 × 10^{-5} ± 8 × 10^{-8} s^{-1}; (b) [**1**] = 0.018 M + $[\mathbf{L}^{HF}]$ = 0.14 M (1:8), k_{obs} = 7.44 × 10^{-5} ± 1 × 10^{-7} s^{-1}; (c) [**1**] = 0.018 M + $[\mathbf{L}^{HF}]$ = 0.22 M (1:12), k_{obs} = 7.36 × 10^{-5} ± 4 × 10^{-7} s^{-1}; (d) [**1**] = 0.018 M + $[\mathbf{L}^{HF}]$ = 0.22 M (1:12) and $[FC_6H_4I]$ = 0.054 M (1:3), k_{obs} = 7.38 × 10^{-5} ± 1.69 × 10^{-7} s^{-1}.

Thus, in this proportion, $\mathbf{L}^{HF}$ performs better to form the corresponding Pd^0 catalyst than XantPhos or PhPEWO-F and about the same as ^{t}BuBrettPhos.[2] The ^{31}P spectra in toluene at 25 °C show independent signals for free $\mathbf{L}^{HF}$ (δ = −11.1 ppm) or coordinated to Pd^0 (δ = 45.6 ppm), and integration supports the composition $Pd(\mathbf{L}^{HF})_3$ for the Pd^0 complex, regardless of the excess of $\mathbf{L}^{HF}$ used, as far as it is ≥3.

It is also worth noting that competing formation of PfH, observed for some other ligands,[1] was not detected in these experiments. Furthermore, an experiment in the presence of 4-fluoroiodobenzene as a reoxidant to prevent formation of $Pd(\mathbf{L}^{HF})_3$ gave the same k_{elim}, demonstrating that the low $\Delta G^{\ddagger}_{Pf-Pf}$ observed is due to the destabilization of the ground state structure with two $\mathbf{L}^{HF}$ ligands and not the stabilization of the Pd^0 complex with an extra ligand.

DOI: 10.1021/acs.organomet.9b00460
Organometallics XXXX, XXX, XXX−XXX

(2) For $[L^{HF}]$:$[PdPf_2(THF)_2]$ = 2:1 or with the isolated complex *cis*-$[PdPf_2(L^{HF})_2]$ (**6**), the evolution shows more complex kinetics. In addition to the coupling product, Pf−Pf, the reaction produces also: (i) isomerization to *trans*-$[PdPf_2(L^{HF})_2]$ (**8**) by a dissociative mechanism,[32] which is more easily accessible for crowded complexes, and (ii) if **6** has been made in situ from **1**, and THF is present in the solution, the reaction regenerates some complex $[PdPf_2(THF)_2]$ (**1**). The latter is as a consequence of the capability of palladium(0) complex $Pd(L^{HF})_2$ to sequester L^{HF}, forming $Pd(L^{HF})_3$, so that some **1** is formed from **6** (Scheme 3). The values obtained from the ^{19}F integrals corresponding to the Pd^0 complex with respect to the internal standard suggest that the number of coordinated phosphines is between 2 and 3. In the presence of 4-fluoroiodobencene as a reoxidant, the fast formation of *trans*-$[Pd(p\text{-}FC_6H_4)I(L^{HF})_2]$ precludes formation of of $Pd(L^{HF})_3$ and also prevents formation of **1** from **6**.

(3) Finally, for $[L^{HF}]$:$[PdPf_2(THF)_2]$ = *n*:**1** with 2 > *n* > 1, a mixture of complexes is formed in solution, which evolves as shown in Figure 8: *cis*-$[PdPf_2(L^{HF})_2]$ (**6**) is consumed

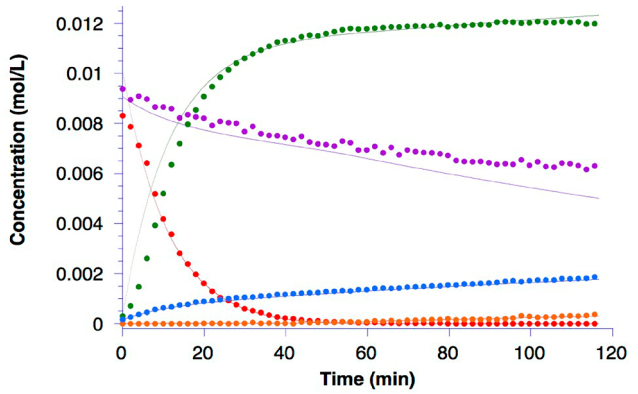

Figure 8. Concentration/time plots (dots) and best least-squares fitting (continuous lines) for the reductive elimination in toluene (0.5 mL) from [**1**] = 0.019 M + $[L^{HF}]$ = 0.030 M (1:1.5) at 298 K, monitored by ^{19}F NMR. Red dots: *cis*-$[PdPf_2(L^{HF})_2]$ (**6**); purple dots: *cis*-$[PdPf_2(L^{HF})(THF)]$ (**7**); green dots: *trans*-$[PdPf_2(L^{HF})_2]$ (**8**); blue dots: Pf−Pf; orange dots: $[PdPf_2(THF)_2]$ (**1**). Colored lines represent the kinetic simulation obtained by fitting the equations optimized with different values for k_{obs} from **6** and for the *functionally three-coordinate species* as a whole.

relatively fast, during the first 30 min, in which Pf−Pf is formed slowly. Also, *cis*-$[PdPf_2(L^{HF})(THF)]$ (**7**), in equilibrium with **6** and L^{HF}, is consumed at a slower rate (Figure 8). The main product of the reaction is *trans*-$[PdPf_2(L^{HF})_2]$ (**8**), and during the experiment, *cis*-$[PdPf_2(THF)_2]$ (**1**) is also formed. Knowing the rate constants for the formation of Pf−Pf from **6** and from **1**, it is possible to calculate k_{obs} for the reductive elimination from **7** (no assumption about the pathway was made); a value k_{obs} = 2.3 × 10^{-5} s^{-1} was obtained. Kinetic simulation visualizes how fast Pf−Pf would be formed if the rates of the reductive elimination were approximately identical for **6** and for **7** (black lines in Figure 8). The rate of formation of Pf−Pf would be noticeably faster than observed experimentally.

In summary, the experimental observations fit well the mechanistic Scheme 3 well and show that, in the absence of excess L^{HF}, which allows for L^{HF} dissociation from **6**, the isomerization of **6** to **8** is faster than the reductive elimination process. The most plausible isomerization mechanism is via a three-coordinate intermediate **7**empty, which means that this intermediate is energetically accessible from the other *functionally three-coordinate species* and that the reductive elimination from **7**empty is not extremely fast. On the other hand, the sum of contributions of all the *functionally three-coordinate species* (the cis species with one L^{HF}) produces (for a ratio of **1**:L^{HF} < 1:1.5) an apparent reductive elimination rate that is less than one-third the coupling rate from the cis species with two L^{HF} (**6**) (2.12 × 10^{-5} vs 7.7 × 10^{-5} s^{-1}). More detailed discussion is available in the SI).

CONCLUSIONS

Ligand L^{HF} is an example of monodentate biphenyl phosphine with a size that still allows for cis coordination to Pd of two phosphines. In the absence of sufficient extra free L^{HF}, there are equilibria of L^{HF} dissociation or displacement by a weak smaller ligand such as THF or OH_2 or by the distal aryl of the biphenyl of the phosphine that remains coordinated. When the two phosphines L^{HF} are coordinated in cis positions, the interligand repulsions close the Pf−Pf angle to about 81.21° and induce a tetrahedral distortion of the square-planar coordination. These two distortions destabilize the ground state, making the reductive elimination transition state more accessible than expected. As a matter of fact, the use of L^{HF} in excess makes it very efficient ($\Delta G^{\ddagger}_{Pf-Pf}$ = 23.1 kcal·mol^{-1}), better than XantPhos or PhPEWO-F and about the same as ^{t}BuBrettPhos.[1]

The tetrahedral distortion caused by overcrowding seems to be an important reason for the easier coupling. This suggests that the design of chelating ligands (not necessarily bulky) forcing tetrahedral distortions at Pd might be catalytically productive. Other studies on structurally related ligands are in progress.

ASSOCIATED CONTENT

Supporting Information

The Supporting Information is available free of charge on the ACS Publications website at DOI: 10.1021/acs.organomet.9b00460.

General methods. Synthesis of new compounds. Determination of rate constants. Other studies in solution. Computational section. Experimental procedure for X-ray crystallography. NMR spectra. IR spectra (PDF)

Accession Codes

CCDC 1938395−1938396 contain the supplementary crystallographic data for this paper. These data can be obtained free of charge via www.ccdc.cam.ac.uk/data_request/cif, or by emailing data_request@ccdc.cam.ac.uk, or by contacting The Cambridge Crystallographic Data Centre, 12 Union Road, Cambridge CB2 1EZ, UK; fax: +44 1223 336033.

AUTHOR INFORMATION

Corresponding Authors

*Tel: (+34)983423231; E-mail: espinet@qi.uva.es. (P.E.)
*Tel: (+34)983184623; E-mail: casares@qi.uva.es; Web: http://cinquima.uva.es. (J.A.C.)

ORCID

María Pérez-Iglesias: 0000-0002-5391-264X
Rebeca Infante: 0000-0002-3754-4189

DOI: 10.1021/acs.organomet.9b00460
Organometallics XXXX, XXX, XXX−XXX

Juan A. Casares: 0000-0001-8833-2066
Pablo Espinet: 0000-0001-8649-239X

Author Contributions

The manuscript was written through contributions of all authors. All authors have given approval to the final version of the manuscript.

Author Contributions

‡M.P.-I. and R.I. contributed equally.

Notes

The authors declare no competing financial interest.

■ ACKNOWLEDGMENTS

Financial support by the Spanish MINECO (CTQ2016-80913-P) and the Junta de Castilla y León (JCyL VA051P17, VA062G18 and M.P.-I. predoctoral grant) is gratefully acknowledged. This paper is dedicated to Prof. Miguel A. Ciriano (University of Zaragoza) on the occasion of his 70th birthday.

■ REFERENCES

(1) Gioria, E.; delPozo, J.; Martínez-Ilarduya, J. M.; Espinet, P. Promoting Difficult Carbon−Carbon Couplings: Which Ligand Does Best? *Angew. Chem., Int. Ed.* **2016**, *55*, 13276−13280.

(2) delPozo, J.; Gioria, E.; Espinet, P. Olefin Insertion Versus Cross-Coupling in trans-[Pd(Ar)X($AsPh_3$)$_2$] Complexes (X = I, F, CF_3) Treated with a Phosphine-EWOlefin Ligand to Induce Ar−X Coupling. *Organometallics* **2017**, *36*, 2884−2890.

(3) Gioria, E.; Martínez-Ilarduya, J. M.; García-Cuadrado, D.; Miguel, J. A.; Genov, M.; Espinet, P. Phosphines with Tethered Electron-Withdrawing Olefins as Ligands for Efficient Pd-Catalyzed Aryl-Alkyl Coupling. *Organometallics* **2013**, *32*, 4255−4261.

(4) Williams, D. B. G.; Shaw, M. L. P-Alkene Bidentate Ligands: An Unusual Ligand Effect in Pd-Catalysed Suzuki Reactions. *Tetrahedron* **2007**, *63*, 1624−1629.

(5) Luo, X.; Zhang, H.; Duan, H.; Liu, Q.; Zhu, L.; Zhang, T.; Lei, A. Superior Effect of a π-Acceptor Ligand (Phosphine-Electron-Deficient Olefin Ligand) in the Negishi Coupling Involving Alkylzinc Reagents. *Org. Lett.* **2007**, *9*, 4571−4574.

(6) Tuxworth, L.; Baiget, L.; Phanopoulos, A.; Metters, O. J.; Batsanov, A. S.; Fox, M. A.; Howard, J. A. K.; Dyer, P. W. Phosphine-Alkene Ligand-Mediated Alkyl-Alkyl and Alkyl-Halide Elimination Processes from Palladium(II). *Chem. Commun.* **2012**, *48*, 10413−10415.

(7) (a) Wolfe, J. P.; Tomori, H.; Sadighi, J. P.; Yin, J.; Buchwald, S. L. Simple, Efficient Catalyst System for the Palladium-Catalyzed Amination of Aryl Chlorides, Bromides, and Triflates. *J. Org. Chem.* **2000**, *65*, 1158−1174. (b) Christmann, U.; Vilar, R.; White, A. J. P.; Williams, D. J. Synthesis of Two Novel Dinuclear Palladium(I) Complexes and Studies of Their Catalytic Activity in Amination Reactions. *Chem. Commun.* **2004**, *4*, 1294−1295. (c) Christmann, U.; Pantazis, D. A.; Benet-Buchholz, J.; McGrady, J. E.; Maseras, F.; Vilar, R. Experimental and Theoretical Investigations of New Dinuclear Palladium Complexes as Precatalysts for the Amination of Aryl Chlorides. *J. Am. Chem. Soc.* **2006**, *128*, 6376−6390. (d) Fors, B. P.; Watson, D. A.; Biscoe, M. R.; Buchwald, S. L. A Highly Active Catalyst for Pd-Catalyzed Amination Reactions. *J. Am. Chem. Soc.* **2008**, *130*, 13552−13554. (e) Milner, P. J.; Maimone, T. J.; Su, M.; Chen, J.; Müller, P.; Buchwald, S. L. Investigating the Dearomative Rearrangement of Biaryl Phosphine-Ligated Pd(II) Complexes. *J. Am. Chem. Soc.* **2012**, *134*, 19922−19934. For recent examples, see: (f) DeAngelis, A. J.; Gildner, P. G.; Chow, R.; Colacot, T. J. Generating Active "L-Pd(0)" via Neutral or Cationic π-Allylpalladium Complexes Featuring Biaryl/Bipyrazolylphosphines: Synthetic, Mechanistic, and Structure−Activity Studies in Challenging Cross-Coupling Reactions. *J. Org. Chem.* **2015**, *80*, 6794−6813. (g) Goutierre, A.-S.; Trinh, H. V.; Larini, P.; Jazzar, R.; Baudoin, O. Comparative Structural Analysis of Biarylphosphine Ligands in Arylpalladium Bromide and Malonate Complexes. *Organometallics* **2017**, *36*, 129−135. (h) Yadav, M. R.; Nagaoka, M.; Kashihara, M.; Zhong, R.-L.; Miyazaki, T.; Sakaki, S.; Nakao, Y. The Suzuki−Miyaura Coupling of Nitroarenes. *J. Am. Chem. Soc.* **2017**, *139*, 9423−9426.

(8) Arrechea, P. L.; Buchwald, S. L. Biaryl Phosphine Based Pd(II) Amido Complexes: The Effect of Ligand Structure on Reductive Elimination. *J. Am. Chem. Soc.* **2016**, *138*, 12486−12493.

(9) Leroux, F. R.; Bonnafoux, L.; Heiss, C.; Colobert, F.; Lanfranchi, D. A. A Practical Transition Metal-Free Aryl-Aryl Coupling Method: Arynes as Key Intermediates. *Adv. Synth. Catal.* **2007**, *349*, 2705−2713.

(10) Olsen, E. P. K.; Arrechea, P. L.; Buchwald, S. L. Mechanistic Insight Leads to a Ligand Which Facilitates the Palladium-Catalyzed Formation of 2-(Hetero)Arylaminooxazoles and 4-(Hetero)-Arylaminothiazoles. *Angew. Chem., Int. Ed.* **2017**, *56*, 10569−10572.

(11) Milne, J. E.; Buchwald, S. L. An Extremely Active Catalyst for the Negishi Cross-Coupling Reaction. *J. Am. Chem. Soc.* **2004**, *126*, 13028−13032.

(12) Mak, A. M.; Jong, H.; Robins, E. G.; Sullivan, M. B.; Lim, Y. H.; Yang, Y.; Johannes, C. W. Mechanistic Insights and Implications of Dearomative Rearrangement in Copper-Free Sonogashira Cross-Coupling Catalyzed by Pd-Cy*Phine. *Organometallics* **2016**, *35*, 1036−1045.

(13) Baba, K.; Tobisu, M.; Chatani, N. Palladium-Catalyzed Direct Synthesis of Phosphole Derivatives from Triarylphosphines through Cleavage of Carbon-Hydrogen and Carbon-Phosphorus Bonds. *Angew. Chem., Int. Ed.* **2013**, *52*, 11892−11895.

(14) (a) Pérez-Rodríguez, M.; Braga, A. A. C.; García-Melchor, M.; Pérez-Temprano, M. H.; Casares, J. A.; Ujaque, G.; de Lera, A. R.; Álvarez, R.; Maseras, F.; Espinet, P. C-C Reductive Elimination in Palladium Complexes, and the Role of Coupling Additives. A DFT Study Supported by Experiment. *J. Am. Chem. Soc.* **2009**, *131*, 3650−3657. (b) Ozawa, F. Reductive elimination. *Fundamentals of Molecular Catalysis* **2003**, *3*, 479. (c) Gillie, A.; Stille, J. K. Mechanisms of 1,1-Reductive Elimination from Palladium. *J. Am. Chem. Soc.* **1980**, *102*, 4933−4941. (d) Ozawa, F.; Ito, T.; Yamamoto, A. Mechanism of thermal decomposition of trans-diethylbis(tertiary phosphine)-palladium(II). Steric effects of tertiary phosphine ligands on the stability of diethylpalladium complexes. *J. Am. Chem. Soc.* **1980**, *102*, 6457−6463.

(15) Choukroun, R.; Lorber, C.; Lepetit, C.; Donnadieu, B. Reactivity of [$Cp_2Ti(CO)_2$] and $B(C_6F_5)_3$: Formation of the Acylborane Complexes [$Cp_2Ti(CO)(\eta^2$-$OCB(C_6F_5)_3)$] and [Cp_2Ti-$(THF)(\eta^2$-$OCB(C_6F_5)_3)$]. *Organometallics* **2003**, *22*, 1995−1997.

(16) Mehta, M.; Garcia de la Arada, I.; Perez, M.; Porwal, D.; Oestreich, M.; Stephan, D. W. Metal-Free Phosphine Oxide Reductions Catalyzed by $B(C_6F_5)_3$ and Electrophilic Fluorophosphonium Cations. *Organometallics* **2016**, *35*, 1030−1035.

(17) Gioria, E.; Martínez-Ilarduya, J. M.; García-Cuadrado, D.; Miguel, J. A.; Genov, M.; Espinet, P. Phosphines with Tethered Electron-Withdrawing Olefins as Ligands for Efficient Pd-Catalyzed Aryl-Alkyl Coupling. *Organometallics* **2013**, *32*, 4255−4261.

(18) Murphy-Jolly, M. B.; Lewis, L. C.; Caffyn, A. J. M. The Synthesis of Tris(Perfluoroalkyl)Phosphines. *Chem. Commun.* **2005**, 4479−4480.

(19) Hierso, J. C. Indirect Nonbonded Nuclear Spin-Spin Coupling: A Guide for the Recognition and Understanding of "through-Space" NMR J Constants in Small Organic, Organometallic, and Coordination Compounds. *Chem. Rev.* **2014**, *114*, 4838−4867.

(20) Contreras, R. H.; Llorente, T.; Ducati, L. C.; Tormena, C. F. Revisiting NMR Through-Space J_{FF} Spin−Spin Coupling Constants for Getting Insight into Proximate F—F Interactions. *J. Phys. Chem. A* **2014**, *118*, 5068−5075.

(21) The through-space coupling between fluorine nuclei is very common. See refs 19 and 20.

(22) Aullon, G.; Ujaque, G.; Lledos, A.; Alvarez, S.; Alemany, P. To Bend or Not To Bend: Dilemma of the Edge-Sharing Binuclear

DOI: 10.1021/acs.organomet.9b00460
Organometallics XXXX, XXX, XXX−XXX

Square Planar Complexes of d8 Transition Metal Ions. *Inorg. Chem.* **1998**, *37*, 804−813.
(23) Pérez-Galán, P.; Delpont, N.; Herrero-Gómez, E.; Maseras, F.; Echavarren, A. M. Metal−Arene Interactions in Dialkylbiarylphosphane Complexes of Copper, Silver, and Gold. *Chem. - Eur. J.* **2010**, *16*, 5324−5332.
(24) Cordero, B.; Gómez, V.; Platero-Prats, A. E.; Revés, M.; Echeverría, J.; Cremades, E.; Barragán, F.; Alvarez, S. Covalent radii revisited. *Dalton Trans.* **2008**, 2832−2838.
(25) Alvarez, S. A Cartography of the van Der Waals Territories. *Dalt. Trans.* **2013**, *42*, 8617−8636.
(26) (a) Espinet, P.; Albéniz, A. C.; Casares, J. A.; Martínez-Ilarduya, J. M. ^{19}F NMR in Organometallic Chemistry. Applications of Fluorinated Aryls. *Coord. Chem. Rev.* **2008**, *252*, 2180−2208. (b) Alonso, M. A.; Casares, J. A.; Espinet, P.; Martínez-Ilarduya, J. M.; Pérez-Briso, C. The 3,5-Dichlorotrifluorophenyl Ligand, a Useful Tool for the Study of Coordination Modes and Dynamic Behavior of Complexes of Palladium and Platinum. *Eur. J. Inorg. Chem.* **1998**, *1998*, 1745−1753. (c) Casares, J. A.; Coco, S.; Espinet, P.; Lin, Y.-S. Observation of a Slow Dissociative Process in Palladium(II) Complexes. *Organometallics* **1995**, *14*, 3058−3067.
(27) Espinet, P.; Echavarren, A. M. The Mechanisms of the Stille Reaction. *Angew. Chem., Int. Ed.* **2004**, *43*, 4704−4734.
(28) Gioria, E. Promoting Difficult Coupling Processes. Synthesis of Phosphine-Olefin Hybrid Ligands, Reactivity and Reductive Elimination Studies. Doctoral Thesis, Universidad de Valladolid, 2018.
(29) Pérez-Rodríguez, M.; Braga, A. A. C. C.; Garcia-Melchor, M.; Pérez-Temprano, M. H.; Casares, J. A.; Ujaque, G.; De Lera, A. R.; Álvarez, R.; Maseras, F.; Espinet, P. C-C Reductive Elimination in Palladium Complexes, and the Role of Coupling Additives. A DFT Study Supported by Experiment. *J. Am. Chem. Soc.* **2009**, *131*, 3650−3657.
(30) Usón, R.; Forniés, J.; Martínez, F.; Tomás, M. Mono- and Bi-Nuclear Anionic Pentafluorophenyl Complexes of Palladium(II) and Platinum(II). *J. Chem. Soc., Dalton Trans.* **1980**, 888−894.
(31) This behavior was studied and reported by us in neat THF as solvent and has been now verified in toluene: Salas, G.; Casares, J. A.; Espinet, P. Enthalpy of Ligand Substitution in Cis Organopalladium Complexes with Monodentate Ligands. *Dalt. Trans.* **2009**, *79*, 8413−8420.
(32) Casado, A. L.; Casares, J. A.; Espinet, P. Mechanism of the Uncatalyzed Dissociative Cis-Trans Isomerization of Bis-(Pentafluorophenyl)Bis(Tetrahydrothiophene): A Refinement. *Inorg. Chem.* **1998**, *37*, 4154−4156.

DOI: 10.1021/acs.organomet.9b00460
Organometallics XXXX, XXX, XXX−XXX